# A ROBUST OPTIMAL GUIDANCE STRATEGY FOR MARS ENTRY

# Emily M. Palmer\* and Anil V. Rao†

A robust optimal guidance strategy is proposed. The guidance strategy is designed to reduce the possibility of violations in inequality path constraints in the presence of modeling errors and perturbations. The guidance strategy solves a constrained nonlinear optimal control problem at the start of every guidance cycle. In order to reduce the possibility of path constraint violations, the objective functional for the optimal control problem is modified at the start of a guidance cycle if it is found that the solution lies within a user-specified threshold of a path constraint limit. The modified objective functional is designed such that it maximizes the margin in the solution relative to the path constraint limit that could potentially be violated in the future. The method is validated on a path-constrained Mars entry problem where the reference model and the perturbed model differ in their atmospheric density. It is found for the example studied that the approach significantly improves the path constraint margin and maintains feasibility relative to a guidance approach that maintains the original objective functional for each guidance update.

# INTRODUCTION

As space exploration continues to progress, Mars has become a subject of great interest. When posed as an optimal control problem, Mars entry, descent, and landing (EDL) is challenging problem due to the path constraints imposed on the vehicle during entry. Beyond satisfying these constraints, it is also necessary to maintain a gap between the the values of the constraint functions relative to the constraint boundaries in order to improve the constraint margins. During entry, it is likely that the actual motion will deviate from the reference (planned) motion due to modeling errors and environmental perturbations. In order for the vehicle to move in such a way that it does not come in close proximity of the constraint boundaries, it is necessary for the guidance command to be robust to these modeling errors and environmental disturbances. This paper provides a demonstration of a method for optimal guidance that reduces sensitivity in the solution to modeling errors and disturbances in order to maintain feasibility and increase path constraint margin during atmospheric entry.

Methods for guidance of aerospace vehicles include linear-quadratic (LQ) methods, <sup>1–3</sup> proportional navigation (PN), <sup>4,5</sup> neighboring optimal control (NOC), <sup>6</sup> and acceleration guidance. <sup>7</sup> These methods, are limited because the guidance law does not take into account the full capability of the vehicle. In addition, these methods are not designed to be robust to modeling errors or perturbations. An approach called desensitized optimal control<sup>8–11</sup> (DOC) has been conceived to improve robustness to modeling errors and environmental disturbances. The goal of DOC is to generate

<sup>\*</sup>Ph.D. Student, Department of Mechanical and Aerospace Engineering, University of Florida, Gainesville, Florida 32611-6250. Email: emilypalmer@ufl.edu.

<sup>&</sup>lt;sup>†</sup>Professor, Department of Mechanical and Aerospace Engineering, University of Florida, Gainesville, FL 32611-6250. E-mail: anilvrao@ufl.edu. Fellow AAS and Associate Fellow AIAA. Corresponding Author

a trajectory that is less sensitive to variations due to modeling errors or other uncertainties in the system. The early work of Ref. 8 provided a foundation for the DOC method. In particular, in Ref. 8 the parameters of interest were elevated to the level of states and the standard optimal control problem is augmented by a sensitivity matrix that captures the sensitivity of the state at an arbitrary time with respect to changes in the initial state. The sensitivity of the state at the terminal time  $t_f$  can then be found with respect to the state at any time t using the chain rule. These sensitivities then can be incorporated into the objective functional. The DOC approach was first formulated for unconstrained optimal control problems, then later developed for problems with control and state constraints. This methodology was used to solve a Mars Entry problem with respect to uncertainty in atmospheric density. One issue with using the sensitivity matrix is that the optimal control problem increases in dimension, with the number of states increasing quadratically as a function of the number of original states and parameters of interest. The increase in dimensionality was later reduced using traditional sensitivity functions.  $^{10}$ 

One fundamental characteristic of DOC is that the entire trajectory is designed with the goal of reducing sensitivity. It is noted, however that increasing the robustness of the entire trajectory decreases overall performance. As a result, it is preferable to focus the increase in robustness to only those aspects of the trajectory where such robustness is advantageous. This research is aimed at reducing the effect of uncertainty and disturbances when the solution lies in close proximity to the constraint limits and maintains the original formulation of the problem when the solution lies far from the constraint limits. While desensitized optimal control often requires manipulation of the state matrix and objective functional, in this paper a method for guidance is developed that reduces computational complexity relative to previous methods for desensitized optimal control. In the approach of this paper, two separate objective functionals are employed: (1) the original objective functional and (2) a modified objective functional that is intended to increase the margin between the value of a path constraint function and the constraint limit. The guidance strategy is then to solve the original optimal control problem in real time when the solution is distant from the constraint limit and switches to solving the modified optimal control problem when the solution lies near a path constraint limit. This approach ensures feasibility throughout the solution, while reducing performance only when necessary in order to maintain feasibility. The approach developed in this paper is demonstrated on a Mars entry guidance problem where the objective is to maximize the terminal altitude subject to a terminal constraint on speed and path constraints on acceleration load, dynamic, pressure, and heating rate. The steps in the method of this paper are given as follows: (1) the reference optimal trajectory is computed using adaptive Gaussian quadrature collocation; (2) the flight is simulated with the optimal control produced from the reference solution over a guidance cycle using a perturbed (off-nominal) model. During each guidance cycle the values of the path constraint functions are evaluated. If it is found that the value of the path constraint function is approaching the path constraint limit and lies within a certain range of this limit, the modified objective functional is used when re-solving the optimal control problem for use on the next guidance cycle. It is noted that the modified objective functional is designed to minimize the maximum path constraint value experienced by the vehicle over the remaining horizon. On the other hand, if the path constraint values do not lie within the user-chosen range of the path constraint limit or are moving away from this limit, then the original objective functional is employed.

#### BOLZA OPTIMAL CONTROL PROBLEM

Without loss of generality, consider the following optimal control problem in Bolza form. Determine the state,  $\mathbf{x}(\tau) \in \mathbb{R}^{n_x}$ , and the control,  $\mathbf{u}(\tau) \in \mathbb{R}^{n_u}$ , on  $\tau \in [-1, +1]$  that minimize the objective functional

$$J = \mathcal{M}(\mathbf{x}(-1), t_0, \mathbf{x}(+1), t_f) + \frac{t_f - t_0}{2} \int_{-1}^{+1} \mathcal{L}(\mathbf{x}(\tau), \mathbf{u}(\tau), t(\tau; t_0, t_f)) d\tau$$
 (1)

subject to the dynamic constraints

$$\frac{d\mathbf{x}}{d\tau} - \frac{t_f - t_0}{2} \mathbf{f}(\mathbf{x}(\tau), \mathbf{u}(\tau), t(\tau; t_0, t_f)) = \mathbf{0},\tag{2}$$

the inequality path constraints

$$\mathbf{c}_{\min} \le \mathbf{c}(\mathbf{x}(\tau), \mathbf{u}(\tau), t(\tau; t_0, t_f)) \le \mathbf{c}_{\max},$$
 (3)

and the boundary conditions

$$\mathbf{b}_{\min} \le \mathbf{b}(\mathbf{x}(-1), t_0, \mathbf{x}(+1), t_f) \le \mathbf{b}_{\max}. \tag{4}$$

It is noted that domain  $t \in [t_0, t_f]$  and the domain  $\tau \in [-1, +1]$  are related via the affine transformation

$$t(\tau; t_0, t_f) = \frac{t_f - t_0}{2} \tau + \frac{t_f + t_0}{2} \tag{5}$$

### LEGENDRE-GAUSS-RADAU COLLOCATION

Consider now the following partition of the Bolza optimal control problem described in Eqs. (1)–(4) into K mesh intervals. First, let  $(T_0,\ldots,T_K)\in[-1,+1]$  be such that  $T_0< T_1<\cdots< T_K$ . Furthermore, let  $T_0=-1$  and  $T_K=+1$ . Finally, let  $\mathcal{S}_k=[T_{k-1},T_k]$ . Next, let  $\mathbf{x}^{(k)}(\tau)$  and  $\mathbf{u}^{(k)}(\tau)$  be the state and control, respectively, in mesh interval  $\mathcal{S}_k$ . The Bolza optimal control problem given in Eqs. (1)–(4) is then formulated as a K mesh interval problem as follows. Minimize the objective functional:

$$J = \mathcal{M}(\mathbf{x}^{(1)}(-1), t_0, \mathbf{x}^{(K)}(+1), t_f) + \frac{t_f - t_0}{2} \sum_{k=1}^K \int_{T_{k-1}}^{T_k} \mathcal{L}(\mathbf{x}^{(k)}(\tau), \mathbf{u}^{(k)}(\tau), t(\tau; t_0, t_f)) d\tau,$$
(6)

subject to the dynamic constraints:

$$\frac{d\mathbf{x}^{(k)}}{d\tau} - \frac{t_f - t_0}{2} \mathbf{f}(\mathbf{x}^{(k)}(\tau), \mathbf{u}^{(k)}(\tau), t(\tau; t_0, t_f)) = \mathbf{0} \quad (k = 1, ..., K)$$
 (7)

the inequality path constraints:

$$\mathbf{c}_{\min} \le \mathbf{c}(\mathbf{x}^{(k)}(\tau), \mathbf{u}^{(k)}(\tau), t(\tau; t_0, t_f)) \le \mathbf{c}_{\max} \quad (k = 1, ..., K)$$
(8)

and the boundary conditions

$$\mathbf{b}_{\min} \le \mathbf{b}(\mathbf{x}^{(1)}(-1), t_0, \mathbf{x}^{(K)}(+1), t_f) \le \mathbf{b}_{\max}.$$
 (9)

It is noted that, in order to maintain continuity at each interior mesh point, the condition  $\mathbf{x}(T_k^-) = \mathbf{x}(T_k^+)$  (k=1,...,K-1) is enforced.

The partitioned optimal control problem given in Eqs. (6)–(9) is discretized using Legendre-Gauss-Radau (LGR) collocation as described in Refs. 12–15. In the LGR method, the state in every mesh interval is approximated as

$$\mathbf{x}^{(k)}(\tau) \approx \mathbf{X}^{(k)}(\tau) = \sum_{j=1}^{N_k+1} \mathbf{X}_j^{(k)} \ell_j^{(k)}(\tau)$$
 (10)

where  $\ell_i^{(k)}(\tau)$  is the basis of Lagrange polynomials

$$\ell_j^{(k)}(\tau) = \prod_{i=1, i \neq j}^{N_k+1} \frac{\tau - \tau_i^{(k)}}{\tau_j^{(k)} - \tau_i^{(k)}}$$
(11)

and  $(\tau_1^{(k)},...,\tau_{N_k}^{(k)})$  are the LGR points in mesh interval  $\mathcal{S}_k$  and  $\tau_{N_k+1}^{(k)}=T_k$  is a noncollocated point. The derivative of the state approximation  $\mathbf{X}^{(k)}(\tau)$  is given as

$$\frac{d\mathbf{X}^{(k)}}{d\tau} = \sum_{j=1}^{N_k+1} \mathbf{X}_j^{(k)} \frac{d\ell_j^{(k)}}{d\tau}$$
 (12)

The dynamic constraints given by Eq. (7) are collocated at the  $N_k$  LGR points in mesh interval  $k \in [1,...,K]$  as

$$\sum_{j=1}^{N_k+1} D_{ij}^{(k)} \mathbf{X}_j^{(k)} - \frac{t_f - t_0}{2} \mathbf{f}(\mathbf{X}_i^{(k)}, \mathbf{U}_i^{(k)}, t_i^{(k)}) = \mathbf{0} \quad (i = 1, ..., N_k)$$
(13)

where  $t_i^{(k)} = t(\tau_i^{(k)}; t_0, t_f)$  and

$$D_{ij}^{(k)} = \left[\frac{d\ell_j^{(k)}}{d\tau}\right]_{\tau=\tau_i}, \ (i=1,\dots,N_K; j=1,\dots,N_{K+1})$$
 (14)

are the elements of the  $N_k \times (N_k+1)$  Legendre-Gauss-Radau differentiation matrix  $k \in [1,...,K]$ . The LGR approximation then leads to the following nonlinear programming problem (NLP). Minimize

$$\mathcal{J} = \mathcal{M}(\mathbf{X}_{1}^{(1)}, t_{0}, \mathbf{X}_{N_{K}+1}^{(K)}, t_{f}) + \sum_{k=1}^{K} \sum_{i=1}^{N_{k}} \frac{t_{f} - t_{0}}{2} w_{j}^{(k)} \mathcal{L}(\mathbf{X}_{i}^{(k)}, \mathbf{U}_{i}^{(k)}, t_{i}^{(k)})$$
(15)

subject to the collocation constraints of Eq. (13), the discretized path constraints

$$\mathbf{c}_{\min} \le \mathbf{c}(\mathbf{X}_{i}^{(k)}, \mathbf{U}_{i}^{(k)}, t_{i}^{(k)}) \le \mathbf{c}_{\max} \quad (i = 1, ..., N_{k}),$$
 (16)

the discretized boundary conditions

$$\mathbf{b}_{\min} \le \mathbf{b}(\mathbf{X}_1^{(1)}, t_0, \mathbf{X}_{N_K+1}^{(K)}, t_f) \le \mathbf{b}_{\max},$$
 (17)

and the continuity constraints

$$\mathbf{X}_{N_k+1}^{(k)} = \mathbf{X}_1^{(k+1)}, \quad (k = 1, ..., K-1).$$
 (18)

#### METHOD ROBUST OPTIMAL GUIDANCE USING LGR COLLOCATION

In this section a method for robust optimal guidance is described. The method developed in this section employs LGR collocation as a guidance algorithm on a *shrinking horizon* using a modification of the method for guidance and control developed in Ref. 16-17. In the method of Ref. 16, following optimal control problem was re-solved at the start of every guidance cycle  $t_0 + k\Delta T$ , where k is the guidance cycle and  $\Delta T$  is the guidance cycle duration. It is noted that the method given in Ref. 16 did not explicitly consider path constraints. In particular, on any guidance it is possible that the optimal control problem may have no solution because disturbances or perturbations may make it such that the path constraints cannot be satisfied given the initial state for that guidance cycle. In order to overcome the issues with path constraints, an approach to guidance is developed that makes it possible to re-solve the optimal control while maintaining feasibility within the path constraints.

The following approach is developed to improve robustness when solving the optimal control problem with path constraints. First, two models for the entry vehicle are used. First, a reference model is used to solve the optimal control problem on the remaining horizon. Second, a perturbed model is used to simulate the dynamics over each guidance cycle. The following strategy is then implemented for optimal guidance. First, the reference optimal solution is generated using LGR collocation using the reference model. Then, using the perturbed (actual) model, the control obtained from LGR collocation is used to simulate the motion of the system over a guidance cycle of duration  $\Delta T$  time units. The perturbed (actual) trajectory obtained using the reference optimal control is referred to as the actual trajectory. The simulated state at the time  $\Delta T$  time units from the start of the guidance cycle produces a state at the end of the guidance cycle, and this state is used as the initial condition when re-solving the optimal control problem over the remaining horizon, that is, from the end of the guidance cycle to  $t_f$ . This process of simulating the motion of the vehicle using the control from  $\mathbb{GPOPS} - \mathbb{II}$  and solving the optimal control problem over the remaining horizon (which in this case is a shrinking horizon as the guidance cycles evolve) is repeated until the remaining horizon is smaller than  $\Delta T$ . Once the remaining horizon is less than  $\Delta T$  time units the optimal control problem is not solved again and the control obtained from the last solution obtained from  $\mathbb{GPOPS} - \mathbb{II}$  is used for the remainder of the flight.

The method of this paper differs from that of Ref. 16 in the following key manner. Specifically, in Ref.  $^{16}$  did not take into account path constraints, whereas the method of this paper includes the path constraints in the solution of the guidance problem. In order to incorporate the path constraints, the optimal control problem is formulated using one of two possible objective functionals. If the solution does not lie in proximity of the path constraint limits then the original optimal control problem is solved. If, however, it is found that the solution on a given guidance cycle is encroaching on a path constraint limit, then a modified objective functional is used that imposes a penalty on the path constraint. Denoting c as the path constraint of interest, four possible cases exist for the solution to lie in proximity of a path constraint limit: (1)  $c_{\rm max}>0$  and  $\dot{c}>0$ ; (2)  $c_{\rm max}<0$  and  $\dot{c}>0$ ; (3)  $c_{\rm min}>0$  and  $\dot{c}<0$ ; and (4)  $c_{\rm min}<0$  and  $\dot{c}<0$ . It is beyond the scope of this paper to develop the modified objective functional for all four cases and, thus, only the case where  $c_{\rm max}>0$  and  $\dot{c}>0$  will be considered here. For this particular case, the following function is used in order to determine if the solution lies within a specified proximity of a path constraint limit:

$$P(t) = \frac{c(\mathbf{x}(t), \mathbf{u}(t), t)}{c_{\text{max}}} \qquad t \in [t_0 + k\Delta T, t_0 + (k+1)\Delta T], \tag{19}$$

where k is the current guidance cycle and c is the scalar path constraint of interest. It is noted in Eq. 19 that P(t) is the fraction of the path constraint limit reached on the current guidance cycle. The maximum value of P(t) is computed and compared to a user-specified threshold,  $\alpha$ , where  $\alpha$  is a fraction of the total allowable path constraint limit. The quantity  $\alpha$  represents the proximity of the path constraint function relative to the path constraint limit, and the value  $\alpha$  is a user-specified parameter. It is only necessary to take action if the path constraint is approaching the path constraint limit. While the method works if the path constraint function lies within the threshold  $\alpha$  for either the lower or upper limit, the discussion here focuses on the case where the path constraint function is approaching its upper limit (as the approach is simply reversed if the path constraint function is approaching its lower limit). Suppose that the percentage of the total allowable value reached is greater than the user chosen percentage and the path is increasing. Then the following two conditions will be satisfied:

$$\max P(t) \ge \alpha \tag{20}$$

and

$$\dot{c} > 0 \tag{21}$$

If the conditions given in Eqs. (20) and 21 are satisfied, then the original objective functional is replaced by a modified objective functional when re-solving the optimal control problem over the remaining horizon. The modified objective functional, denoted  $J_2$ , is designed to increase the margin between the value of the path constraint function and the path constraint limit. This improvement in margin is achieved by minimizing the maximum value of the path constraint function over the remaining horizon which is equivalent to minimizing

$$\lim_{p \to \infty} \left( \int_a^b f^p(t)dt \right)^{1/p}. \tag{22}$$

While using Eq. (22) as the objective functional is not computationally tractable, it is possible to approximate Eq. (22) using a finite and relatively small value of p. Then the modified objective functional is given as

$$\left(\int_{t_0}^{t_f} f^p(t)dt\right)^{1/p} \tag{23}$$

where p is an even number and is kept relatively small (for example p might take on the value of four or six). In order to reduce the size of the integral in Eq. (22), the path constraints of interest are scaled by the maximum allowable value which leads to the following modified objective functional

$$J_2 = \min\left(\int_{t_0}^{t_f} \left(\frac{c(t)}{c_{\text{max}}}\right)^p dt\right)^{1/p} \tag{24}$$

If the conditions listed in Eq. (20)-(21) are not met, then the original objective functional, which is defined as  $J_1$  is used when re-solving the optimal control problem.

#### MARS ENTRY OPTIMAL CONTROL PROBLEM

In this section the Mars entry optimal control problem of interest is formulated. First, the equations of motion for a point mass over a spherical nonrotating planet are given as 18

$$\dot{r} = v \sin \gamma, 
\dot{v} = -D - g \sin \gamma, 
\dot{\theta} = \frac{v \cos \gamma \sin \psi}{r \cos \phi}, 
\dot{\phi} = \frac{v \cos \gamma \cos \psi}{r}, 
\dot{\gamma} = \frac{1}{v} \left[ L \cos \sigma + \left( \frac{v}{r} - \frac{g}{v} \right) \cos \gamma \right], 
\dot{\psi} = \frac{L \sin \sigma}{v \cos \gamma} + \frac{v \cos \gamma \sin \psi \tan \theta}{r},$$
(25)

where r is the radial distance above the center of Mars, v is the speed,  $\theta$  is the latitude,  $\phi$  is the longitude,  $\gamma$  is the flight path angle,  $\psi$  is the heading angle, and  $g = \mu/r^2$ . Next, the lift and drag specific forces are given, respectively, as

$$L = \frac{qC_LS}{m},$$

$$D = \frac{qC_DS}{m},$$
(26)

where  $C_L$  is the coefficient of lift,  $C_D$  is the coefficient of drag, S is the characteristic length, m is the vehicle mass,  $q = \rho v^2/2$  is the dynamic pressure,  $\rho = \rho_0 \exp(-h/H)$  is the atmospheric density, where, h = r - R is the altitude. It is noted that  $\rho_0$ , H, and R are the Martian sea level density, the density scale height, and the radius of the planet, respectively. The physical constants used in the study are given in 1. During entry, the vehicle is subject to path constraints on the

Value Quantity Value Quantity R $3.386 \times 10^{6} \text{ m}$  $0.6 \, \mathrm{m}$  $r_n$  $4.284 \times 10^{13} \text{ m}^3/\text{s}^2$ 3 M $\mu$  $9.80665 \text{ m/s}^2$ N0.5  $g_0$ S $15.9 \text{ m}^2$  $1.9027 \times 10^{-8} \text{ W/cm}^2$  $K_a$  $C_D$ 9354 m1.45 H0.348 $0.0158 \text{ kg/m}^3$  $C_L$  $\rho_0$ 3300 kgm

Table 1. Physical constants.

dynamic pressure, the sensed acceleration, and the heating rate. Denoting the acceleration load as  $A = \sqrt{L^2 + D^2}$  and the heating rate as  $\dot{Q} = K_q \left(\frac{\rho}{r_n}\right)^N v^M \leq \dot{Q}_{\max}$ , these constraints are given,

respectively, as

$$q \leq q_{\text{max}},$$
 (27)

$$A \leq A_{\max}, \tag{28}$$

$$\dot{Q} \leq \dot{Q}_{\text{max}},$$
 (29)

where N, M, and  $K_q$  are constants, and  $g_0$  is the Earth sea level acceleration due to gravity. Next, the initial state and time are fixed and these initial values are provided in Table 2. The final state is free with the exception of the final speed which is fixed. Additionally, bounds placed on the control,  $\sigma$ . Finally, limits on the state are provided in Table 3. The objective is to maximize the altitude at the terminus of the entry, that is, minimize

$$\min J_1 = -r(t_f). \tag{30}$$

Quantity	Value	Quantity	Value
$r_0$	$3.5112 \times 10^6 \text{ m}$	$\theta_0$	0 rad
$v_0$	6000 m/s	$\phi_0$	-0.0873  rad
$\gamma_0$	-0.2007  rad	$\psi_0$	1.6581 rad

Table 2. Boundary conditions.

Table 3	Rounds on	variables ar	nd constraints.
Table 5.	Dounds on	variables ar	iu consu amis.

540 m/s

Quantity	Value	Quantity	Value
$r_{\min}$	$3.3862 \times 10^6 \text{ m}$	$r_{ m max}$	$3.5112\times10^6~\mathrm{m}$
$v_{ m min}$	0.1 m/s	$v_{ m max}$	6000 m/s
$ heta_{\min}$	$-2\pi$ rad	$\theta_{ m max}$	$2\pi$ rad
$\phi_{ m min}$	-1.2217  rad	$\phi_{ m max}$	1.2217 rad
$\gamma_{ m min}$	-1.0472  rad	$\gamma_{\rm max}$	0 rad
$\psi_{ m min}$	$-2\pi$ rad	$\psi_{\mathrm{max}}$	$2\pi$ rad
$\sigma_{ m min}$	0.05236 rad	$\sigma_{ m max}$	2.0944 rad
$q_{\mathrm{min}}$	0 Pa	$q_{\max}$	10000 Pa
$A_{\min}$	$0 \text{ m/s}^2$	$A_{\max}$	$5g_0 \text{ m/s}^2$
$Q_{\min}$	0 W/cm <sup>2</sup>	$Q_{\max}$	70 W/cm <sup>2</sup>

# OPTIMAL CONTROL PROBLEM SOLVER

 $v_f$ 

All optimal solutions in this paper were generated using the optimal control software  $\mathbb{GPOPS}-\mathbb{II}$  an hp adaptive Gaussian quadrature collocation solver.  $^{12-14,19-23}$  The hp method allows for smaller meshes to be utilized than typical h methods (fixed-order methods), yet still achieves the desired accuracy tolerances. This is achieved by concentrating mesh points where the solution is nonsmooth and rapidly changing and placing fewer mesh points where the solution is smooth. The decay of the Legendre polynomial coefficients as a function of the coefficient index was used to determine the

smoothness of the solution.  $^{23}$  GPOPS – II implements the nonlinear problem solver, IPOPT, an interior point method. IPOPT was employed in full Newton mode and supplied with the objective function gradient, Lagrangian Hessian, and the constraint Jacobian. The first and second derivatives were calculated from sparse central finite differencing. The boundary conditions, model parameters, an initial guess, an initial mesh, and functions defining the dynamic constraints as well as the objective functional were used as inputs to GPOPS – II. GPOPS – III then outputs the optimal solution, containing the control matrix and corresponding state matrix.

# **RESULTS**

In this section the aforementioned robust optimal guidance strategy is demonstrated on the Mars entry optimal control problem defined earlier. The objective functional for the reference optimal control problem is given in Eq. (30), while the modified objective functional is given in Eq. (24) using the value p=4. The trajectories obtained using the robust optimal guidance strategy are compared against the reference solution. In order to demonstrate the robust optimal guidance strategy, the reference and the perturbed models differ in the density model used. The reference and perturbed density models are given, respectively, as

$$\rho = \rho_0 \exp(-h/H), \tag{31}$$

$$\rho = \tilde{\rho}_0 \exp(-h/H), \tag{32}$$

where  $\rho_0$  and  $\tilde{\rho}_0$  are the reference and perturbed surface level densities, h is the altitude, and H is the density scale height. When simulating a modeling error, two different cases will be presented. The first modeling error consists of a constant five percent difference between  $\rho_0$  and  $\tilde{\rho}_0$ , while the second modeling error is drawn from a uniform distribution on each guidance cycle on the interval  $[\rho_0, 1.05\rho_0]$ . All results were obtained for  $\alpha=0.9$  (that is, the threshold where the objective functional is changed is when the path constraint function lies within ten percent of the upper limit on the path constraint), Additionally, a guidance cycle duration  $\Delta T=10$  s is chosen.

# **Constant 5% Error in Surface Level Density**

Table 4 shows the components of the final state along with the maximum path constraint function values for for the case where the the perturbed surface level density is five percent higher than the nominal surface level density (that is, the case where  $\tilde{\rho}_0 = 1.05\rho_0$ ). It can be seen from Table 4 that the robust guidance method developed in this paper not only prevents the flight from violating the constraints, but it also produces a final altitude that is closer in value to the final altitude obtained from the reference optimal solution when compared with the guidance strategy that does not use switch objective functionals. Additionally, it is noted that the for the robust guidance method developed in this paper, the modified objective functional was used on only two guidance cycles but still keeps the path constraints from being violated. Furthermore, Fig. 3 shows that the robust guidance strategy developed in this paper does not drastically increase computational complexity and follows a similar trajectory as a guidance strategy that employs only the original objective functional, where computational time generally decreases as the problem is being resolved each cycle. Finally, again from Table 4, it is seen that the terminal time obtained using the robust guidance strategy is quite similar to the terminal time obtained on the reference optimal solution.

Table 4. Final state and maximum path values

Quantity	Reference Solution	Guidance with only $J_1$	Guidance with $J_1$ or $J_2$
$h(t_f)$	10.43 km	10.84 km	10.46 km
$v(t_f)$	540 m/s	538 m/s	539 m/s
$\theta(t_f)$	0.306 rad	0.299 rad	0.308 rad
$\phi(t_f)$	-0.137  rad	$-0.135  {\rm rad}$	-0.137  rad
$\gamma(t_f)$	-0.246  rad	-0.243  rad	$-0.254  \mathrm{rad}$
$\psi(t_f)$	2.07 rad	2.07 rad	2.06 rad
$t_f$	316.4 s	309.7 s	369. s
$q_{ m max}$	6.825 KPa	6.918 KPa	6.606 KPa
$A_{\max}$	$5.00g_0 \text{ m/s}^2$	$5.07g_0 \text{ m/s}^2$	$4.84g_0 \text{ m/s}^2$
$Q_{\max}$	66.2 W/cm <sup>2</sup>	69.4 W/cm <sup>2</sup>	68.9 W/cm <sup>2</sup>

Guidance with  $J_1$  or  $J_2$ Reference Solution
Guidance with only  $J_1$ Guidance with  $J_1$  or  $J_2$ Reference Solution
Guidance with only  $J_1$  $\begin{array}{c} \text{Sbeed (m/s)} \\ \text{2000} \\ \text{3000} \\ \end{array}$ Altitude (km) 150 200 Time (s) 150 200 Time (s) (a) h(t) vs. t. (b) v(t) vs. t.

Figure 1. Altitude and speed using a +5 % error in the atmospheric density

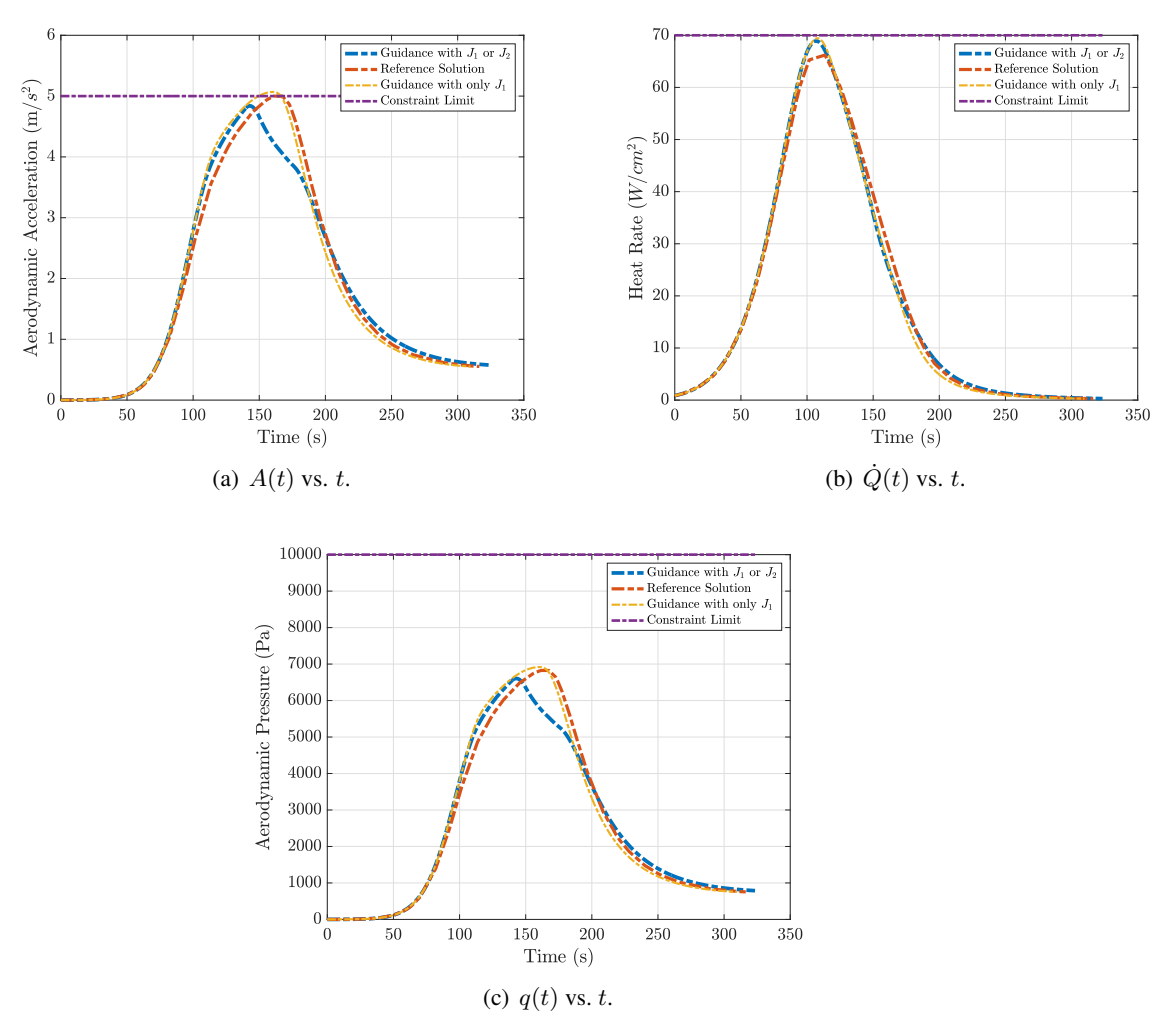


Figure 2. Path constraint values using a +5 % error in the atmospheric density.

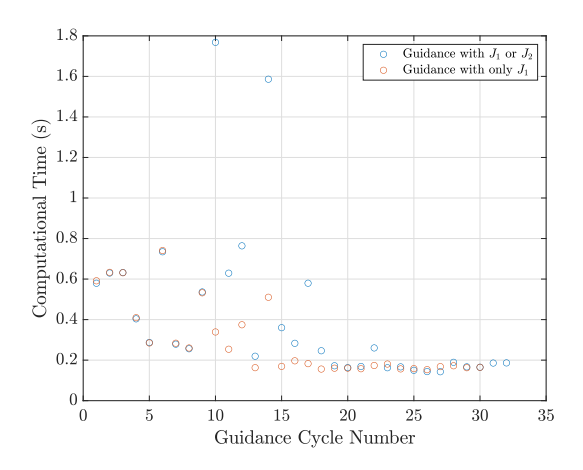


Figure 3. Computation time when re-solving the optimal control problem at each guidance cycle.

### **Random Perturbation in Surface Level Density**

As stated earlier, for the case of a random perturbation, the value of the surface level density at the start of each guidance cycle was drawn from a uniform distribution on  $[\rho_0, 1.05\rho_0]$ . It should be noted that the actual realizations of the random sequence of values of  $\tilde{\rho}_0$  differs every time the guidance simulation is performed (due to the use of a random number generator) which in turn produces different results for each realization. While the random number generator can be seeded to produce the same sequence each time, such an approach is beyond the scope of this paper. Therefore, in this section the results obtained for one realization of a sequence of values of  $\tilde{\rho}_0$  is shown in order to see the effect of using a random perturbation in surface level density. In particular, it is seen from Fig. 5(a) that the robust guidance method described in this paper is able to avoid path constraint violations. Furthermore, as with the constant offset in surface level density, in this case the guidance method switched the objective functional twice throughout the guidance updates. Additionally, from Fig. it is seen that the computational times are of the same order of magnitude as seen in the previous section and generally decrease as the horizon shrinks. While the results obtained in this paper are for a single realization of random values of surface level density, a thorough analysis using Monte Carlo simulation is required in order to obtain a more accurate assessment of the approach described in this paper. Such a Monte Carlo analysis is, however, beyond the scope of this paper.

Table 5. Final state and maximum path values

		•
Quantity	Reference Solution	Guidance with $J_1$ or $J_2$
$ \begin{array}{c} \hline h(t_f) \\ v(t_f) \\ \theta(t_f) \\ \phi(t_f) \\ \gamma(t_f) \end{array} $	10.43 km 540 m/s 0.306 rad -0.137 rad -0.246 rad	10.26 km 539.2 m/s 0.310 rad -0.138 rad -0.256 rad
$\psi(t_f)$ $t_f$ $q_{ m max}$ $A_{ m max}$ $Q_{ m max}$	$2.07  ext{ rad}$ $316.4  ext{ s}$ $6.825  ext{ KPa}$ $5g_0  ext{ m/s}^2$ $66.2  ext{ W/cm}^2$	2.07  rad 325.2  s 6.54  KPa $4.79g_0 \text{ m/s}^2$ $69.04 \text{ W/cm}^2$

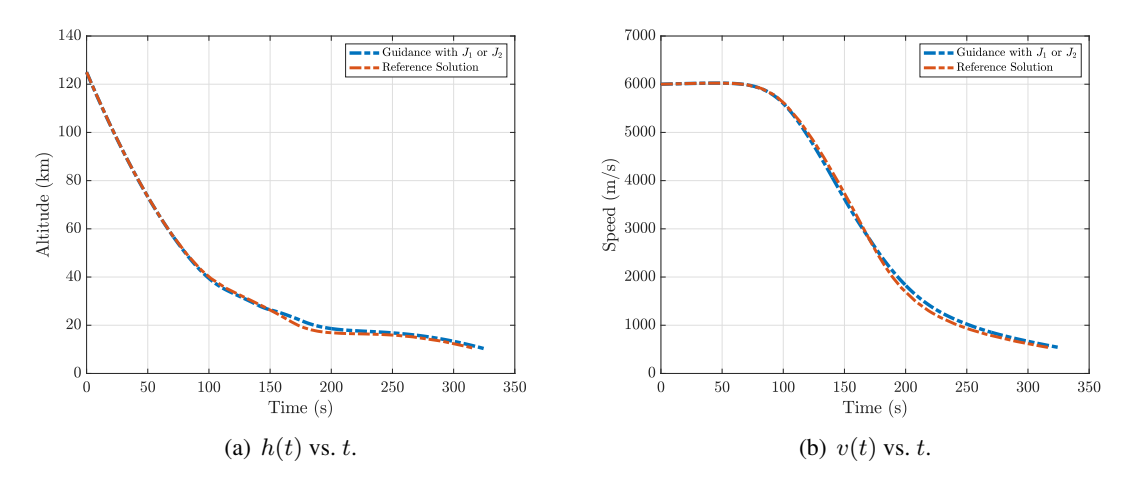


Figure 4. Altitude and speed using a time varying error in the atmospheric density

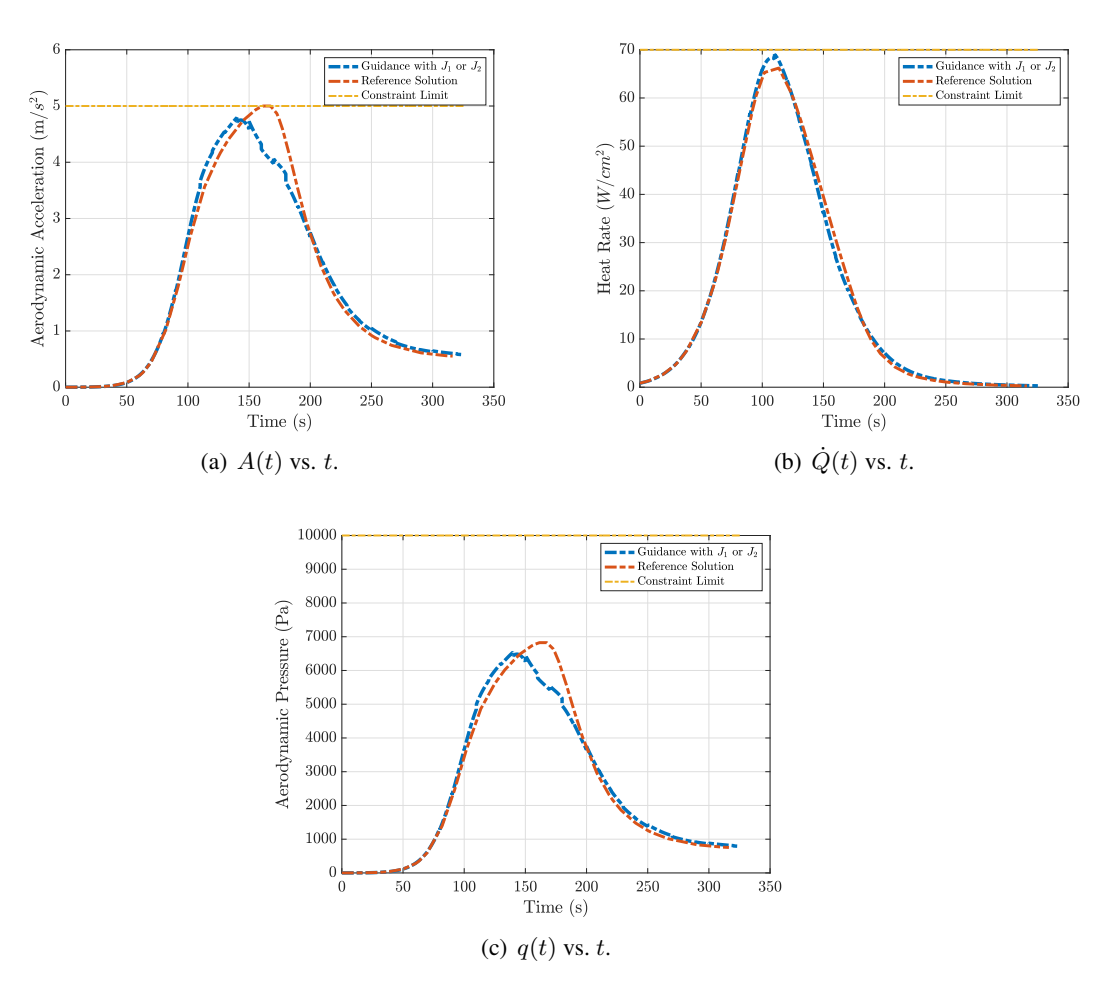


Figure 5. Path constraint values using a time varying error in the atmospheric density.

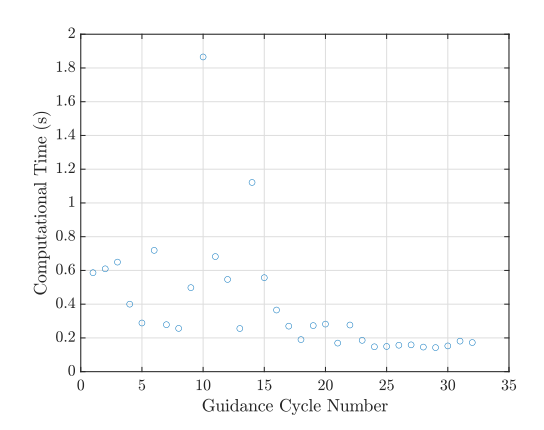


Figure 6. Computational time when re-solving the optimal control problem at each guidance cycle

### **CONCLUSIONS**

An robust optimal guidance method has been proposed and applied to path-constrained a Mars entry problem. The goal was to implement real-time optimal control using mid-course corrections to guide the vehicle in the presence of modeling errors and perturbations. Feasibility was ensured by preventing path constraint violations with the newly developed optimal guidance strategy. In particular, the possibility of maintaining feasibility has been improved by switching the objective functional in the optimal control problem when the solution lies within a user-specified threshold of a path constraint limit. This alternative objective functional is designed to maximize the margin between the path constraint function value and the path constraint limit. In order to demonstrate the approach, two cases of an altitude maximization Mars entry problem have been considered. The first case is one where the reference surface level density is is offset by a constant five percent in the perturbed model, while the second case is one where the surface level density is drawn from a uniform distribution. For both cases considered the objective functional needed to be switched on only two guidance cycles, and for both cases the guidance strategy maintained feasibility with respect to the path constraints. On the other hand, when the objective functional was not switched, the acceleration load limit was violated. The approach developed in this paper appears to be a viable method for improving robustness in optimal guidance.

#### ACKNOWLEDGMENTS

The authors gratefully acknowledge support for this research from the U.S. National Science Foundation under grant CMMI-2031213 and from the U.S. Air Force Research Laboratory under contract FA8651-21-F-1041.

### REFERENCES

- [1] M. Kim and K. V. Grider, "Terminal Guidance for Impact Attitude Angle Constrained Flight Trajectories," *IEEE Transactions on Aerospace and Electronic Systems*, Vol. AES-9, November 1973, pp. 852–859. https://doi.org/10.1109/TAES.1973.309659, 10.1109/TAES.1973.309659.
- [2] A. Farooq and D. J. N. Limebeer, "Optimal Trajectory Regulation for Radar Imaging Guidance," Journal of Guidance, Control, and Dynamics, Vol. 31, July-August 2008, pp. 1076–1092. https://doi.org/10.2514/1.31441.
- [3] V. Shaferman and T. Shima, "Linear Quadratic Guidance Laws for Imposing a Terminal Intercept Angle," *Journal of Guidance, Control, and Dynamics*, Vol. 31, September–October 2008, pp. 1400–1412. https://doi.org/10.2514/1.32836.
- [4] P. Zarchan, *Tactical and Strategic Missile Guidance*, Vol. 239. Reston, VA: Progress in Astronautics and Aeronautics, AIAA, 6 ed., 2012.
- [5] X. Liu, Z. Shen, and P. Lu, "Closed-Loop Optimization of Guidance Gain for Constrained Impact," Journal of Guidance, Control, and Dynamics, Vol. 40, February 2017, pp. 453–460. https://doi. org/10.2514/1.G000323.
- [6] M. R. Jardin and A. E. B. Jr., "Neighboring Optimal Aircraft Guidance in Winds," *Journal of Guidance, Control, and Dynamics*, Vol. 24, July–August 2001, pp. 710–715. https://doi.org/10.2514/2.4798.
- [7] J. C. Harpold and C. A. Graves, "Shuttle Entry Guidance," *Journal of the Astronautical Sciences*, Vol. 27, No. 3, 1981, pp. 239–268.
- [8] H. Seywald and R. Kumar, "Desensitized optimal trajectories," Vol. 93, jan 1996, pp. 103–113.
- [9] S. Li and Y. Peng, "Mars entry trajectory optimization using DOC and DCNLP," *Advances in Space Research*, Vol. 47, Feb. 2011, pp. 440–452, 10.1016/j.asr.2010.09.005.
- [10] V. Makkapati, M. Dor, et al., "Trajectory Desensitization in Optimal Control Problems," 2018 IEEE Conference on Decision and Control (CDC), Institute of Electrical and Electronics Engineers (IEEE), dec 2018, 10.1109/CDC.2018.8619577.
- [11] K. Seywald and H. Seywald, "Desensitized Optimal Control," *AIAA Scitech 2019 Forum*, American Institute of Aeronautics and Astronautics, jan 2019, 10.2514/6.2019-0651.
- [12] D. Garg, M. A. Patterson, W. W. Hager, A. V. Rao, D. A. Benson, and G. T. Huntington, "A Unified Framework for the Numerical Solution of Optimal Control Problems Using Pseudospectral Methods," *Automatica*, Vol. 46, November 2010, pp. 1843–1851. DOI: 10.1016/j.automatica.2010.06.048.
- [13] D. Garg, W. W. Hager, and A. V. Rao, "Pseudospectral Methods for Solving Infinite-Horizon Optimal Control Problems," *Automatica*, Vol. 47, April 2011, pp. 829–837. DOI: 10.1016/j.automatica.2011.01.085.
- [14] D. Garg, M. A. Patterson, C. L. Darby, C. Francolin, G. T. Huntington, W. W. Hager, and A. V. Rao, "Direct Trajectory Optimization and Costate Estimation of Finite-Horizon and Infinite-Horizon Optimal Control Problems via a Radau Pseudospectral Method," *Computational Optimization and Applications*, Vol. 49, June 2011, pp. 335–358. DOI: 10.1007/s10589–00–09291–0.
- [15] M. A. Patterson, W. W. Hager, and A. V. Rao, "A ph mesh refinement method for optimal control," *Optimal Control Applications and Methods*, Vol. 36, July–August 2015, pp. 398–421, 10.1002/oca.2114.
- [16] M. E. Dennis, W. W. Hager, and A. V. Rao, "Computational Method for Optimal Guidance and Control Using Adaptive Gaussian Quadrature Collocation," *Journal of Guidance, Control, and Dynamics*, Vol. 42, Sept. 2019, pp. 2026–2041, 10.2514/1.G003943.
- [17] E. M. Palmer and A. V.Rao, "Mars Entry Optimal Trajectory Generation, Guidance, and Control," AIAA Scitech 2022 Forum, American Institute of Aeronautics and Astronautics, jan 2022, 10.2514/6.2022-2390.
- [18] J. T. Betts, Practical Methods for Optimal Control and Estimation Using Nonlinear Programming. SIAM, 2010.
- [19] C. L. Darby, W. W. Hager, and A. V. Rao, "An hp-Adaptive Pseudospectral method for Solving Optimal Control Problems," *Optimal Control Applications and Methods*, Vol. 32, Aug. 2010, pp. 476–502, 10.1002/oca.957.

- [20] C. L. Darby, D. Garg, and A. V. Rao, "Costate Estimation using Multiple-Interval Pseudospectral Methods," *Journal of Spacecraft and Rockets*, Vol. 48, Sept. 2011, pp. 856–866, 10.2514/1.a32040.
- [21] M. A. Patterson and A. V. Rao, "GPOPS-II," ACM Transactions on Mathematical Software, Vol. 41, oct 2014, pp. 1–37, 10.1145/2558904.
- [22] F. Liu, W. W. Hager, and A. V. Rao, "Adaptive mesh refinement method for optimal control using nonsmoothness detection and mesh size reduction," *Journal of the Franklin Institute*, Vol. 352, oct 2015, pp. 4081–4106, 10.1016/j.jfranklin.2015.05.028.
- [23] F. Liu, W. W. Hager, and A. V. Rao, "Adaptive Mesh Refinement Method for Optimal Control Using Decay Rates of Legendre Polynomial Coefficients," *IEEE Transactions on Control Systems Technology*, Vol. 26, July 2018, pp. 1475–1483, 10.1109/tcst.2017.2702122.